BJR

Received: 26 October 2015 | Revised: 23 December 2015 | Accepted: 12 January 2016

doi: 10.1259/bjr.20150896

Cite this article as:
Ozaki K, Matsui O, Kobayashi S, Minami T, Kitao A, Gabata T. Morphometric changes in liver cirrhosis: aetiological differences correlated with progression. *Br J Radiol* 2016; **89**: 20150896.

FULL PAPER

Morphometric changes in liver cirrhosis: aetiological differences correlated with progression

[1]KUMI OZAKI, MD, PhD, [1]OSAMU MATSUI, MD, PhD, [2]SATOSHI KOBAYASHI, PhD, [1]TETSUYA MINAMI, MD, PhD, [1]AZUSA KITAO, MD, PhD and [1]TOSHIFUMI GABATA, MD, PhD

[1]Department of Radiology, Kanazawa University Graduate School of Medical Science, Kanazawa, Japan
[2]Department of Quantum Medicine Technology, Kanazawa University Graduate School of Medical Science, Kanazawa, Japan

Address correspondence to: Dr Kumi Ozaki
E-mail: *ozakik@staff.kanazawa-u.ac.jp*

Objective: To evaluate the morphometric changes in liver cirrhosis using multidetector CT volumetry and to analyse the differences in morphometric changes among different aetiologies and stages of cirrhosis.
Methods: Each portal segment with the respective proportion relative to total liver volume was measured in 54 patients without cirrhosis as a control (male/female, 29/25; 62.4 ± 7.6 years) and 250 patients with cirrhosis (male/female, 172/78; 64.6 ± 9.2 years) related to hepatitis virus infection ($n = 96$), alcoholism ($n = 88$) and non-alcoholic steatohepatitis (NASH) ($n = 66$). 149 patients were classified as patients with Child–Pugh Class A, 57 patients as patients with Class B and 44 patients as patients with Class C. The Kruskal–Wallis test was used for statistical analysis ($p < 0.05$).
Results: Cirrhosis associated with all aetiologies commonly showed atrophy of the medial and anterior segments and right lobe and hypertrophy of the lateral segment and caudate lobe compared with the control ($p < 0.05$). In Child–Pugh Class A, hypertrophy of the caudate lobe progressed more in alcoholism and NASH than in virus-related aetiologies ($p < 0.001$). Hypertrophy of the lateral segment and atrophy of the medial and anterior segments and right lobe progressed less in NASH than in cases with virus related and alcoholic cirrhosis ($p < 0.001$). In patients with Class B, these differences were less prominent than in those with Class A ($p < 0.001$). In Class C, no significant differences were noted in any segment, regardless of aetiology ($p > 0.05$).
Conclusion: Morphometric changes of cirrhosis display different patterns according to aetiology. Differences between aetiologies would decrease with progression of cirrhosis.
Advances in knowledge: Morphometric changes of cirrhosis display different patterns according to aetiology. Differences between aetiologies would decrease with progression of cirrhosis.

INTRODUCTION

Liver cirrhosis is the end stage of a variety of chronic diffuse liver diseases and is irreversibly progressive, leading to hepatic dysfunction, portal hypertension and hepatocellular carcinoma. It is a major public health problem worldwide.[1] Therefore, identifying the causative factors and quantifying the stage and/or activity of liver cirrhosis are important clinically. To achieve this, liver biopsy is most commonly used as the reference standard for assessing liver fibrosis. Although liver biopsy is a relatively safe procedure, there are various procedure-related risks such as intra-abdominal bleeding, associated with a mortality rate of 1 in 10,000–12,000.[2,3] In addition, it also is subject to inherent risks that include interobserver variability and sampling errors.[4] Therefore, other non-invasively supporting information can be useful in clinical setting, although imaging is unlikely to completely replace liver biopsy in the management algorithm of patients with chronic liver disease in the near future, despite the advances in CT techniques.

Various kinds of morphometric changes are well known to occur in diffuse liver diseases, especially in liver cirrhosis, and they are important for the imaging diagnosis, estimation of severity and understanding of the pathophysiology of the underlying aetiologies. For the objective evaluation of these morphometric changes, conventional cross-sectional imaging by multidetector CT (MDCT) or MR imaging is essential.[5–14] Furthermore, recent advances in MDCT have made it possible to obtain rapid volumetric scanning and three-dimensional reconstruction and provided a new method for precisely measuring liver volume and evaluating intrahepatic vascular structures.[6,7]

Morphometric changes of liver cirrhosis on imaging commonly include atrophy of the medial segment and right lobe

and hypertrophy of the lateral segment and caudate lobe.[6–14] Although several reports have shown that morphometric variations of hepatic segments in cirrhosis differ depending on the aetiologies of cirrhosis,[15] these reports focused mainly only on a part of a segment such as the caudate lobe and analysed only virus-related or alcoholic cirrhosis, while most of them lumped together various aetiologies.[8–14] In addition to differences related to the underlying aetiology, morphometric changes may also depend on the progression of cirrhosis.[5]

The purpose of this study was to evaluate the morphometric changes in liver cirrhosis using MDCT volumetry and to analyse the differences in morphometric changes among different aetiologies, namely virus-, alcoholism-, non-alcoholic steatohepatitis (NASH)-related differences and different stages of liver cirrhosis.

METHODS AND MATERIALS

Patients

This retrospective study was approved by the institutional ethics committee, and informed consent for use of the CT images and clinical data for scientific research purposes was obtained from all patients.

Our study focused on virus-induced (hepatitis B or C), alcoholic and NASH-related cirrhosis because of the high worldwide prevalence of these conditions. Consecutive patients with cirrhosis due to alcoholism ($n = 66$) and NASH ($n = 88$) between October 2005 and December 2009 and 96 consecutive patients with cirrhosis due to hepatitis C or B virus infection between April 2008 and December 2009 who underwent upper abdominal dynamic CT at our institution were enrolled. Preliminarily, we excluded patients with overlap in aetiologies [hepatitis B and C ($n = 18$), hepatitis C and alcoholism ($n = 7$) and hepatitis B and alcoholism ($n = 5$)]. All cases with cirrhosis were pathologically confirmed by percutaneous liver biopsy. Between January 2009 and December 2009, 54 patients who were age and sex matched with clinically diagnosed normal liver (no findings indicating liver disease or diabetes mellitus based on blood tests and imaging diagnosis within 3 months and patient history) and who had undergone dynamic CT were selected as a control group. The inclusion criteria for all patients were as follows: (a) older than 40 years; (b) space-occupying lesions in the liver < 3 cm in diameter and < 3 in number; (c) no history of surgical procedures including transarterial chemoembolization and/or radiofrequency ablation; (d) absence of the below-mentioned anatomic variations of the major intrahepatic portal veins; and (e) availability of good contrast images permitting automatic volumetric analyses.

172 males and 78 females with a mean age of 66.1 years ± 10.1 (mean ± standard deviation) (range, 40–87 years) in the cirrhosis group and 29 males and 25 females with a mean age of 62.4 years ± 7.6 (range, 41–75 years) in the control group were enrolled. In the cirrhosis group, 149 patients were classified as patients with Child–Pugh Class A, 57 patients as patients with Class B and 44 patients as patients with Class C.

Table 1. Clinical features of patients

Variable	Control group	Child–Pugh Class A				Child–Pugh Class B				Child–Pugh Class C			
		Virus	Alcoholism	NASH	*p*-value	Virus	Alcoholism	NASH	*p*-value	Virus	Alcoholism	NASH	*p*-value
Number of cases	54	54	51	44		23	18	16		19	19	6	
Male/female	29/25	36/18	47/4	15/29	<0.001	13/10	18/0	10/6	–	16/3	14/5	3/3	0.237
Overall age (years)	62.4 ± 7.6	65.3 ± 9.4	63.1 ± 9.6	66.3 ± 11.3	0.214	63.9 ± 10.8	67.3 ± 8.3	64.6 ± 8.9	0.257	61.9 ± 9.5	63.9 ± 9.5	63.5 ± 6.7	0.876
Age of male (years)	62.9 ± 8.3	63.1 ± 9.9	63.6 ± 8.3	60.3 ± 11.4	0.498	60.5 ± 9.6	64.6 ± 8.9	65.2 ± 8.0	0.351	60.3 ± 9.5	63.4 ± 9.7	60.0 ± 6.0	0.650
Age of female (years)	61.8 ± 6.9	69.7 ± 6.5	56.5 ± 20.3	69.4 ± 10.1	0.053	68.3 ± 11.2	–	70.7 ± 8.1	0.745	70.3 ± 3.8	65.4 ± 9.5	67.0 ± 6.2	0.688
Body surface area (m^2)	1.64 ± 0.16	1.61 ± 0.21	1.62 ± 0.21	1.62 ± 0.20	0.111	1.70 ± 0.21	1.71 ± 0.16	1.73 ± 0.17	0.197	1.69 ± 0.11	1.72 ± 0.25	1.67 ± 0.11	0.422

NASH, non-alcoholic steatohepatitis.
The data of age and body surface area (BSA) are expressed as means ± standard deviations. *p*-value expressed the value between the control group and three aetiologies in each Child–Pugh Class. The patients with alcoholic cirrhosis showing Child–Pugh Class A and B stage demonstrated a significantly higher proportion of males than females ($p < 0.05$). Neither age nor BSA distribution significantly differed among patients with different aetiologies in any Child–Pugh Class or control group ($p > 0.05$).

Definition of hepatic segments and anatomical exclusion criteria

In standard portal vein anatomy, the main portal vein typically divides at the hepatic hilus into the left and right portal veins. The left portal vein supplies the lateral segment and medial segment. The right portal vein divides into the right anterior trunk that supplies the anterior segment and the right posterior trunk that supplies the posterior segment.[16] The feeding branches into the caudate lobe directly arise from the main portal trunk, left and right portal veins or posterior branch.[17] Patients with variations different from the above-mentioned most common portal anatomical patterns were excluded, because these anatomic variations may result in specific morphometric changes in cirrhosis, which could potentially bias the analysis.

Imaging techniques

Abdominal dynamic CT images were obtained with a LightSpeed VCT® 64 (GE Medical Systems, Milwauke, WI). Images were acquired through the liver in a craniocaudal direction with a 0.625×64 beam collimation. Other CT parameters were as follows: Auto mA (10–700 mA, noise index of 8.0; GE Healthcare); 120 kVp; detector collimation, 2.5 mm; table speed, 14 mm per rotation; gantry rotation time, 0.5 s; reconstruction section thickness of 2.5 mm and reconstruction interval, 2.5 mm. Following pre-contrast CT, a dynamic contrast study was performed using the Smart Prep option (GE Medical Systems), and 600 mgI kg^{-1} of non-ionic contrast material (iomeprol, Iomeron 350; Eisai, Tokyo, Japan) was administered for 30 s. The arterial phase scanning was initiated just after a 200 Hounsfield unit enhancement threshold was achieved in the aorta at the level of the celiac artery. The portal and equilibrium-phase scanning was performed at 35-s and 115-s delays, respectively, from the time of initiation of arterial-phase scanning.

Body surface area measurement

Body surface area (BSA) was calculated using Du Bois and Du Bois's formula {BSA = [0.0061 × BH (cm) + 0.0124 × BW (kg)]},[18] using body weight and body height recorded at the time of the CT examination to explore the possibility that the data might be modified by differences in this parameter.

Figure 1. Bar graphs show total liver volume and total liver volume per body surface area (BSA) among control group and three aetiologies in each Child–Pugh Class. Total liver volume and total liver volume per BSA were significantly larger in patients with alcoholic liver cirrhosis with Child–Pugh Class A stage than in those with other aetiologies and control group ($p < 0.001$). On the other hand, no significant differences were observed among the three aetiologies in Child–Pugh Class B or C. Total liver volume and total liver volume per BSA significantly decreased with progression of cirrhosis in all patients, regardless of aetiology ($p < 0.05$). The data are expressed as means ± standard deviations. *$p < 0.05$ with multiple comparison tests. NASH, non-alcoholic steatohepatitis.

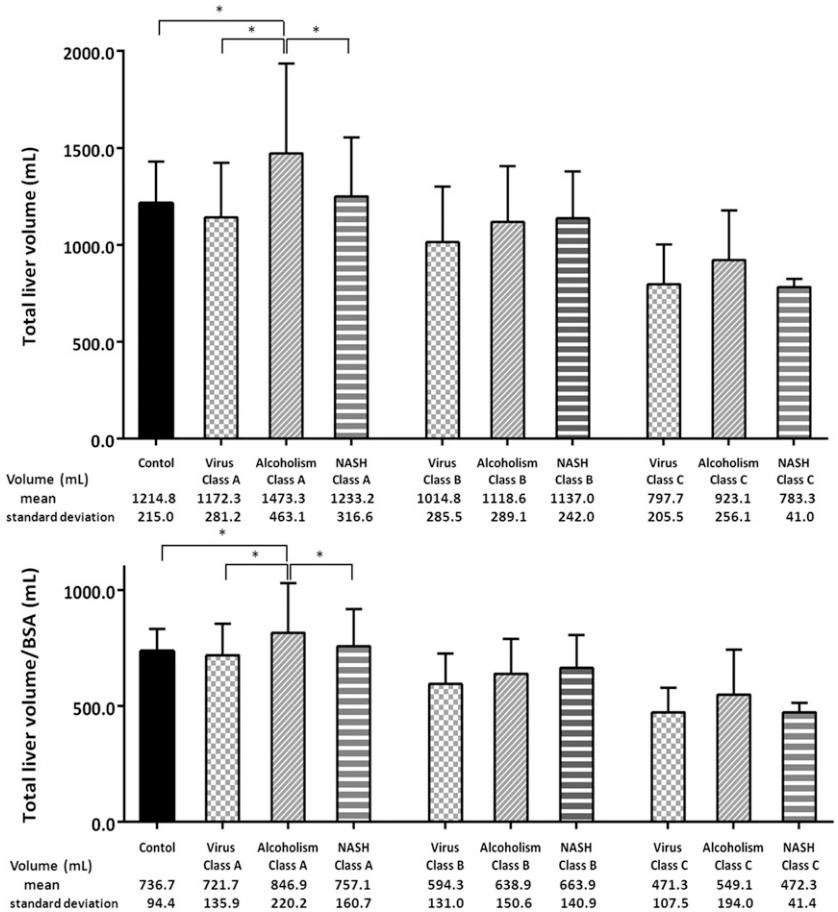

Table 2. Volume and volume ratio of each segment

Segment/lobe	Control	Child–Pugh Class A			Child–Pugh Class B			Child–Pugh Class C		
		Virus	Alcoholism	NASH	Virus	Alcoholism	NASH	Virus	Alcoholism	NASH
Number of patients	54	54	51	44	23	18	16	19	19	6
Lateral segment										
Volume (ml)	205.8 ± 47.0	325.9 ± 98.8	403.8 ± 168.1	278.8 ± 88.0	309.0 ± 107.0	364.6 ± 122.8	300.6 ± 50.5	208.2 ± 79.9	263.5 ± 136.6	193.1 ± 71.7
Proportion (%)	17.2 ± 3.8	28.5 ± 4.8	27.6 ± 7.5	22.6 ± 4.4	30.7 ± 7.2	32.0 ± 3.2	24.8 ± 4.5	25.9 ± 6.6	28.2 ± 8.4	24.6 ± 8.8
p-values		<0.001	<0.001	<0.001	<0.001	<0.001	<0.001	<0.001	<0.001	0.011
Medial segment										
Volume (ml)	178.6 ± 43.8	132.9 ± 47.7	173.6 ± 73.6	162.8 ± 48.8	107.7 ± 24.7	118.6 ± 34.8	140.3 ± 31.1	88.7 ± 19.1	110.8 ± 44.4	90.5 ± 28.9
Proportion (%)	14.7 ± 2.8	11.5 ± 3.6	11.7 ± 2.6	13.2 ± 1.8	10.8 ± 1.8	9.9 ± 3.1	13.4 ± 2.2	11.5 ± 2.6	12.4 ± 4.7	12.6 ± 3.3
p-values		<0.001	<0.001	<0.001	<0.001	<0.001	<0.001	0.001	0.026	0.049
Anterior segment										
Volume (ml)	438.6 ± 101.2	284.7 ± 83.6	351.5 ± 145.5	346.0 ± 117.3	242.0 ± 83.0	245.9 ± 72.2	297.9 ± 88.6	–		
Proportion (%)	35.9 ± 3.8	24.1 ± 4.3	23.7 ± 5.8	27.9 ± 4.7	23.7 ± 2.9	23.8 ± 4.6	27.1 ± 4.7			
p-values		<0.001	<0.001	<0.001	<0.001	<0.001	<0.001			
Posterior segment										
Volume (ml)	328.5 ± 79.8	287.1 ± 94.8	360.3 ± 147.7	300.3 ± 99.0	249.3 ± 116.8	276.4 ± 109.0	254.8 ± 69.2	–		
Proportion (%)	27.0 ± 4.2	25.2 ± 4.3	24.3 ± 6.3	24.3 ± 5.0	24.2 ± 6.1	24.7 ± 6.7	22.2 ± 4.1			
p-values		0.103	0.021	0.029	0.067	0.204	0.004			
Caudate lobe										
Volume (ml)	63.3 ± 14.6	111.8 ± 38.8	184.8 ± 66.3	145.7 ± 52.0	112.1 ± 30.6	149.9 ± 31.0	141.8 ± 29.7	90.6 ± 23.5	120.4 ± 42.7	100.8 ± 21.7
Proportion (%)	5.2 ± 0.9	9.3 ± 2.4	12.8 ± 3.4	12.0 ± 3.8	11.1 ± 1.1	13.7 ± 4.2	12.6 ± 2.1	11.6 ± 2.5	12.9 ± 2.1	12.8 ± 2.3
p-values		<0.001	<0.001	<0.001	<0.001	<0.001	<0.001	<0.001	<0.001	<0.001
Right lobe										
Volume (ml)	767.1 ± 163.9	571.8 ± 164.5	711.8 ± 267.7	646.3 ± 193.5	491.3 ± 188.1	522.3 ± 165.6	552.7 ± 145.0	411.9 ± 141.7	433.4 ± 165.0	398.8 ± 81.2
Proportion (%)	62.9 ± 5.4	49.8 ± 6.3	47.5 ± 9.9	52.2 ± 6.5	46.3 ± 8.4	49.2 ± 10.0	48.9 ± 9.3	52.1 ± 8.4	45.9 ± 12.8	50.4 ± 12.3
p-values		<0.001	<0.001	<0.001	<0.001	<0.001	<0.001	<0.001	<0.001	0.002

NASH, non-alcoholic steatohepatitis.

The data of the volume and the proportion are expressed as means ± standard deviations. *p*-value expressed the multiple pairwise comparisons between different aetiologies in each Child–Pugh class and control group. Morphometric changes associated with all aetiologies commonly showed atrophy of the medial segment and right lobe and hypertrophy of the caudate lobe and lateral segment in Child–Pugh Class A, B and C compared with control group ($p < 0.05$).

Volumetry of the entire liver and hepatic segments

The volumes of the total liver, lateral, medial, anterior and posterior segments and the caudate lobe were measured in all patients; however, in patients with Child–Pugh Class C, discrimination between the anterior and posterior segments was difficult because of poorer visualization of intrahepatic portal veins, and only the volume of the right lobe was measured.

All volumetric measurements were automatically performed using a method similar to that outlined in previous reports[6,7,19,20] with a workstation (Virtual Place Lexus; AZE, Tokyo, Japan). In this method, the following steps were conducted as follows: first, the liver margins on the portal-phase source images were defined using an algorithm for optimal boundary detection in real time; second, the portal veins on portal-phase source images were segmented using a region-growing algorithm with automatically determined thresholds; third, portal veins were separated and analysed; and fourth, the vascular territories were automatically determined and volumetrically calculated based on individual portal branches.[20] Results of the determined area were presented using surface-shaded display and volume-rendering techniques. The peripheral small portal veins were carefully identified by observing the successive slices. Data processing was carried out by two radiologists (KO and OM with 11 and 30 years' experience in abdominal radiology) by consensus.

Figure 2. Box plot showing the proportion of each segment to the total liver volume of the three aetiologies in Child–Pugh Class A. The proportion of the lateral segment to the total liver was significantly smaller in patients with non-alcoholic steatohepatitis (NASH) than in those with virus-related ($p < 0.001$) and alcoholic cirrhosis ($p < 0.001$), the proportion of the medial segment was significantly larger in the patients with NASH than in those with virus-related ($p = 0.021$) and alcoholic cirrhosis ($p = 0.049$), the proportion of the anterior segment was significantly larger in patients with NASH than in those with virus-related ($p = 0.004$) and alcoholic cirrhosis ($p < 0.001$) and the proportion of the caudate lobe was significantly smaller in patients with virus-related cirrhosis than in those with NASH ($p < 0.001$) and alcoholic liver cirrhosis ($p < 0.001$). In addition, the proportion of the right lobe to the total liver was significantly larger in patients with NASH than in those with alcoholic liver cirrhosis ($p < 0.001$). There was no significant difference in the proportion of the posterior segment to the total liver in patients with the three different aetiologies ($p > 0.05$). Shaded boxes indicate the ranges of measured values between the 25th and 75th percentiles, horizontal lines inside boxes indicate medians and the vertical bars (whiskers) indicate values of the 5th and 95th percentiles. The data are expressed as means ± standard deviations. *$p < 0.05$ with multiple comparison tests. These descriptions apply to all of the box plots.

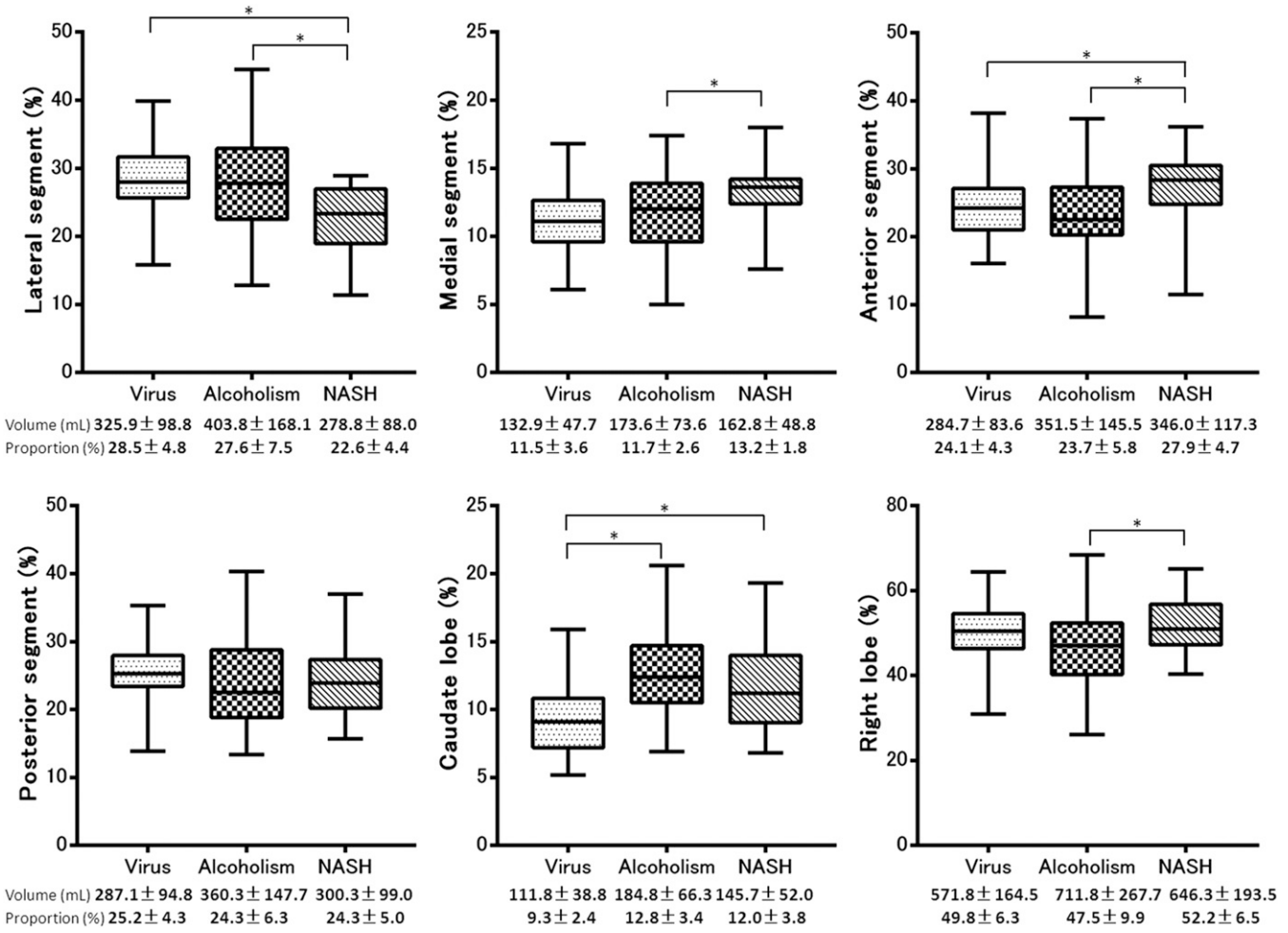

Figure 3. Comparison of portal phase of axial CT images in a 49-year-old woman with normal liver (control group) (a), in a 55-year-old man with virus-related cirrhosis (b), in a 54-year-old man with alcoholic cirrhosis (c) and in a 52-year-old woman with non-alcoholic steatohepatitis (NASH)-related cirrhosis (d) in Child–Pugh Class A. Virus-related (b), alcoholic (c) and NASH-related (d) cirrhosis show atrophy of the medial (white asterisks) and anterior segments and right lobe (white dots) and hypertrophy of the lateral segment (black asterisks) and caudate lobe (black dots) as compared with the control group by multiple comparisons. In particular, the differences in the atrophy of the medial segment and hypertrophy of the caudate lobe among the aetiologies are easily understandable in axial CT images.

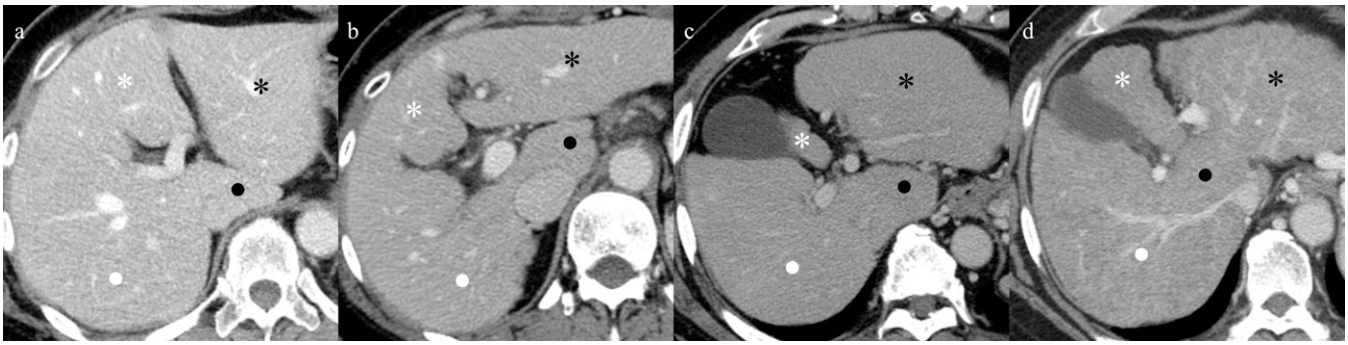

To allow for differences among individuals, the total liver volume per BSA ratio was calculated.[7] The volume of the right lobe was calculated by the sum of the anterior and posterior segments, except for in Child–Pugh Class C. The proportion of each area relative to the total liver was calculated by dividing the volume of each hepatic area by the total liver volume.

Statistical analysis

The distribution of sex in each Child–Pugh Class in the three aetiologies and control group was analysed using χ^2 test, while the significance of differences in age, BSA, total liver volume, total liver volume per BSA and each proportion was analysed using the Kruskal–Wallis test. When a significant difference among groups was identified, multiple pairwise comparisons were performed using Wilcoxon rank sum test with Bonferroni adjustments. As a secondary analysis, changes in total liver volume and total liver volume per BSA in each aetiology in different stages of cirrhosis were also analysed using the Kruskal–Wallis test. p-values < 0.05 were considered to indicate statistical significance. All analyses were performed with statistical software (Dr. SPSS II for Windows, v. 11.0.1 J; IBM Corp., New York, NY; formerly SPSS Inc., Chicago, IL.

RESULTS

Clinical features of patients with liver cirrhosis classified according to the aetiology and stage and patients without definite diffuse liver diseases (control group) are summarized in Table 1. Patients with alcoholic cirrhosis showing Child–Pugh Class A and B stage demonstrated a significantly higher proportion of males than females ($p < 0.05$). Neither age nor BSA distribution significantly differed among patients with different aetiologies in any Child–Pugh Class or the control group ($p > 0.05$).

Total liver volume and total liver volume per BSA were significantly larger in patients with alcoholic liver cirrhosis with Child–Pugh Class A stage than in those with other aetiologies and the control group ($p < 0.001$). On the other hand, no significant differences were observed among the three aetiologies in Child–Pugh Class B or C. Total liver volume and total liver volume per BSA significantly decreased with progression of cirrhosis in all patients with each aetiology ($p < 0.05$) (Figure 1).

The volume and volume ratio of each segment and the results of multiple pairwise comparisons among the patients with different aetiologies in each Child–Pugh Class and control group are summarized in Table 2. Morphometric changes associated with all aetiologies commonly included atrophy of the medial segment and right lobe and hypertrophy of the lateral segment and caudate lobe in Child–Pugh Class A, B and C compared with control group ($p < 0.05$). The results of the multiple pairwise comparisons between each aetiology are summarized in Figures 2, 4 and 6. In patients with Child–Pugh Class A, the proportion of the lateral segment to the total liver in patients with NASH was significantly smaller than that in patients with virus-related ($p < 0.001$) or alcoholic cirrhosis ($p < 0.001$), the proportion of the medial segment in patients with NASH was significantly larger than that in patients with virus-related ($p = 0.021$) and alcoholic cirrhosis ($p = 0.049$), the proportion of the anterior segment in patients with NASH was significantly larger than that in patients with virus-related ($p = 0.004$) and alcoholic cirrhosis ($p < 0.001$) and the proportion of the caudate lobe in patients with virus-related cirrhosis was significantly smaller than that in patients with NASH ($p < 0.001$) and alcoholic liver cirrhosis ($p < 0.001$). In addition, the proportion of the right lobe to the total liver was significantly larger in patients with NASH than in patients with alcoholic liver cirrhosis ($p < 0.001$). There was no significant difference in the proportion of the posterior segment to the total liver among patients with the three different aetiologies ($p > 0.05$) (Figures 2 and 3). In patients with Child–Pugh Class B, the proportion of the lateral segment to the total liver was significantly smaller in patients with NASH than in those with alcoholic cirrhosis ($p < 0.001$), the proportion of the medial segment was significantly larger in patients with NASH than in those with alcoholic cirrhosis ($p = 0.045$), the proportion of the anterior segment was significantly larger in patients with NASH than in those with alcoholic cirrhosis ($p = 0.003$) and the proportion of the caudate lobe was significantly smaller in patients with virus-related cirrhosis than in

those with alcoholic liver cirrhosis ($p = 0.001$). The proportion of the posterior segment and right lobe to the total liver did not differ significantly among patients with the three different aetiologies ($p > 0.05$) (Figures 4 and 5). In patients with Child–Pugh Class C, the proportion of each segment to the total liver did not show significant differences among patients with the three different aetiologies ($p > 0.05$) (Figures 6 and 7).

DISCUSSION

Our findings demonstrate that alcoholic cirrhosis in Child–Pugh Class A induces a significant enlargement of the total liver volume, even after accounting for the effect of male-predominant distribution. On the other hand, no significant differences were seen in the total liver volume or in the distributions of age and BSA between the control and virus- and NASH-related cirrhosis. The total liver volume significantly decreased with progression of cirrhosis, regardless of aetiology. The average volume of the normal livers was similar to that reported in other Asian populations when considering differences in age and race,[6,7] as analysed by volumetric evaluation by MDCT. As reported by Ozaki et al,[6] cirrhosis in Child–Pugh Class A did not necessarily show any reduction in the entire liver volume, in spite of internal complexity of atrophy and hypertrophy. The enlargement noted in alcoholic cirrhosis was similar to that described in a previous report,[21] and our results showed that total liver volume decreased in parallel with progression of the cirrhosis not only in virus-related[6,7] but also alcoholic and NASH-related cirrhosis.

Concerning the volumetric analysis of the portal segments of cirrhosis, several earlier reports concerning virus-related and alcoholic cirrhosis revealed actual atrophy of the medial segment and right lobe and hypertrophy of the lateral segment and caudate lobe in our study.[6,7,10,15] We for the first time revealed that NASH-related cirrhosis showed the same patterns of

Figure 4. Box plot showing the proportion of each segment to the total liver volume of the three aetiologies in Child–Pugh Class B. The proportion of lateral segment to the total liver was significantly smaller in patients with non-alcoholic steatohepatitis (NASH) than in those with alcoholic cirrhosis ($p < 0.001$), the proportion of the medial segment was significantly larger in patients with NASH than in those with alcoholic cirrhosis ($p = 0.045$), the proportion of the anterior segment was significantly larger in the patients with NASH than in those with alcoholic cirrhosis ($p = 0.003$) and the proportion of the caudate lobe was significantly smaller in the patients with virus-related cirrhosis than in those with alcoholic liver cirrhosis ($p = 0.001$). There were no significant differences in the proportion of the posterior segment and right lobe to the total liver among the patients with the three different aetiologies ($p > 0.05$).

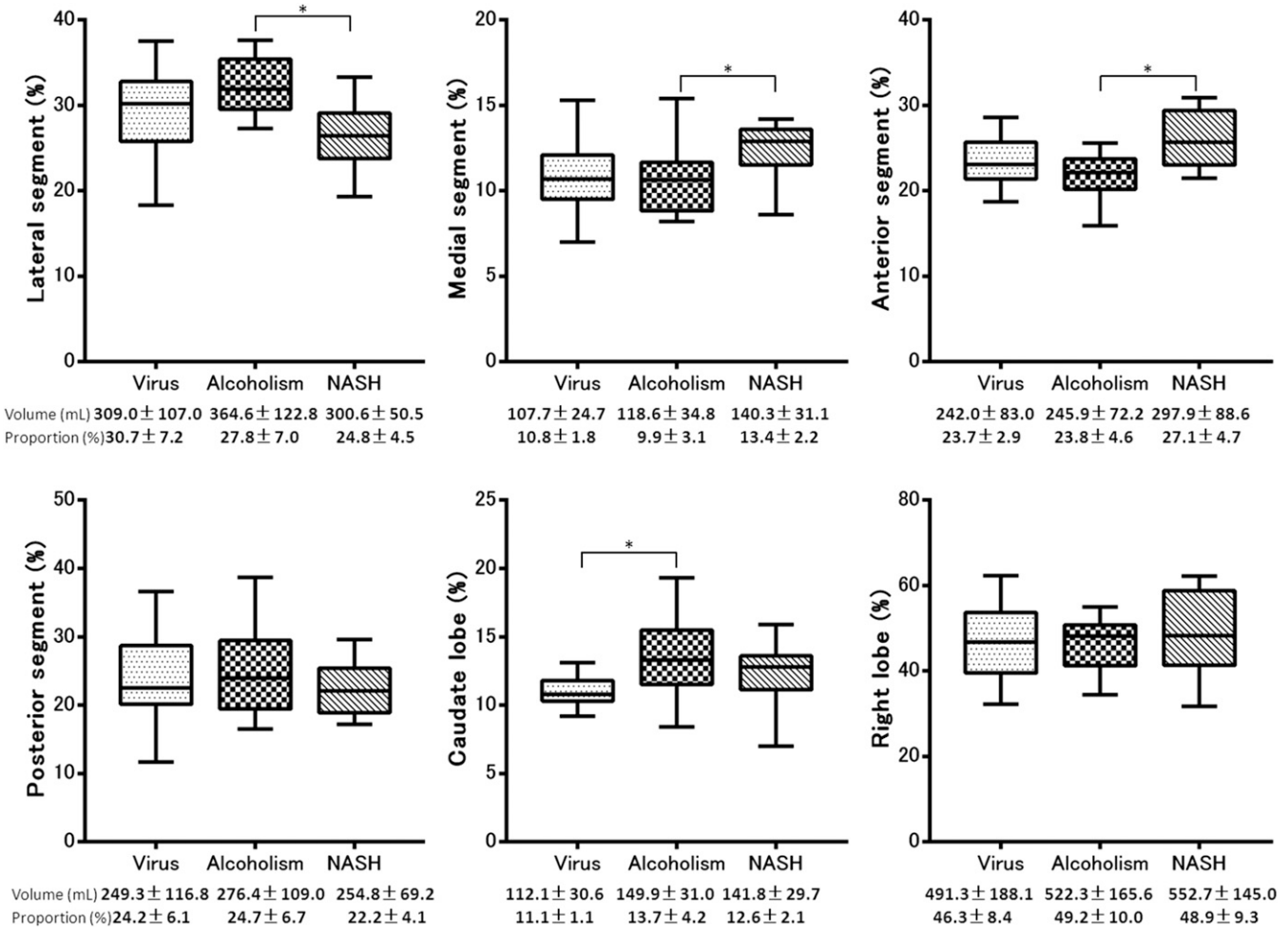

Figure 5. Comparison of portal phase of axial CT images in a 56-year-old woman with virus-related cirrhosis (a), in a 58-year-old man with alcoholic cirrhosis (b) and in a 51-year-old woman with non-alcoholic steatohepatitis (NASH)-related cirrhosis (c) in Child–Pugh Class B. Representative cases of virus-related (a), alcoholic (b) and NASH-related (c) cirrhosis show atrophy of the medial (white asterisks) and anterior segments and right lobe (white dots) and hypertrophy of the lateral segment (black asterisks) and caudate lobe (black dots). The magnitude of the differences between aetiologies was less marked than that of Child–Pugh Class A.

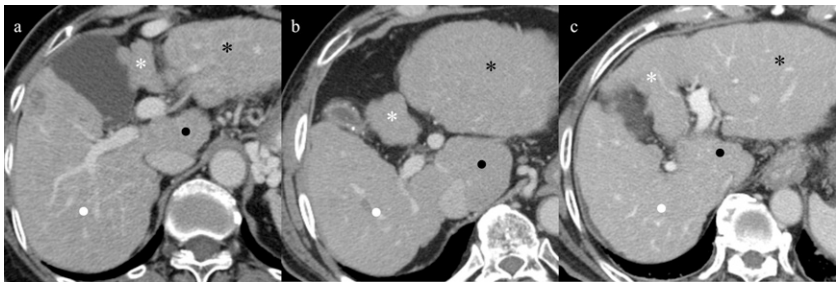

volumetric changes as that seen with virus-related and alcoholic cirrhosis. In addition, our results showed obvious differences among aetiologies and stages of cirrhosis. The distinct hypertrophy of the caudate lobe in alcoholic cirrhosis is the same as that noted in a previous study.[15] In patients with NASH classified as patients with Child–Pugh Class A, these morphometric changes other than hypertrophy of the caudate lobe progressed less than in those with virus-related and alcoholic cirrhosis. The hypertrophy of the caudate lobe progressed more than in patients with virus-related cirrhosis, as well as in patients with alcoholic cirrhosis. In patients with Child–Pugh Class B, these significant differences were less prominent than in those with Child–Pugh Class A , with specifically no significant difference existing between virus- and NASH-related cirrhosis. Cirrhosis in Child–Pugh Class C displayed no significant difference in any segment among the three aetiologies.

The morphometric changes seen in diffuse liver diseases may be closely related to the alteration of intrahepatic haemodynamics caused by cirrhosis-specific pathogenic conditions such as fibrosis, inflammation, regeneration and/or degeneration and others. Although fibrosis is a common change in cirrhosis, its histological pattern varies, depending on the underlying aetiology.[22] For example, the fibrous septa bridging portal triads and central veins are often seen in viral infection-related cirrhosis. On the other hand, cholestasis-induced liver injury shows biliary interface hepatitis including fibroplasia in the portal area, while perivenular and perisinusoidal fibrosis is commonly seen in alcoholic and NASH-related cirrhosis.[23] In addition, there are some histopathological differences between alcoholic and NASH-related cirrhosis,[24] and the distinct amount of histological fibrosis promoted by the metabolic effects of alcohol in alcoholic cirrhosis.[25] These characteristic histological findings of fibrosis, depending on the aetiology of cirrhosis, can be depicted by imaging.[26–28] Furthermore, progressive hepatic fibrosis evokes the so-called regenerative nodules in cirrhosis.[29]

Cirrhosis is classified as macronodular, micronodular and mixed nodular based on the size of regenerative nodules, with this also tending to depend on aetiology.[30] Therefore, the changes occurring in intrahepatic haemodynamics owing to compression by specific histological structures such as regenerative nodules and fibrosis may also differ among aetiologies, and these blood flow disturbances may strongly influence morphometric changes.

In compensated cirrhosis, the selective atrophic area caused by a specific histological structure is compensated for by hypertrophy

Figure 6. Box plot showing the proportion of each segment to the total liver volume of the three aetiologies in Child–Pugh Class C. The proportion of each segment to the total liver did not show significant differences among patients with the three different aetiologies. NASH, non-alcoholic steatohepatitis.

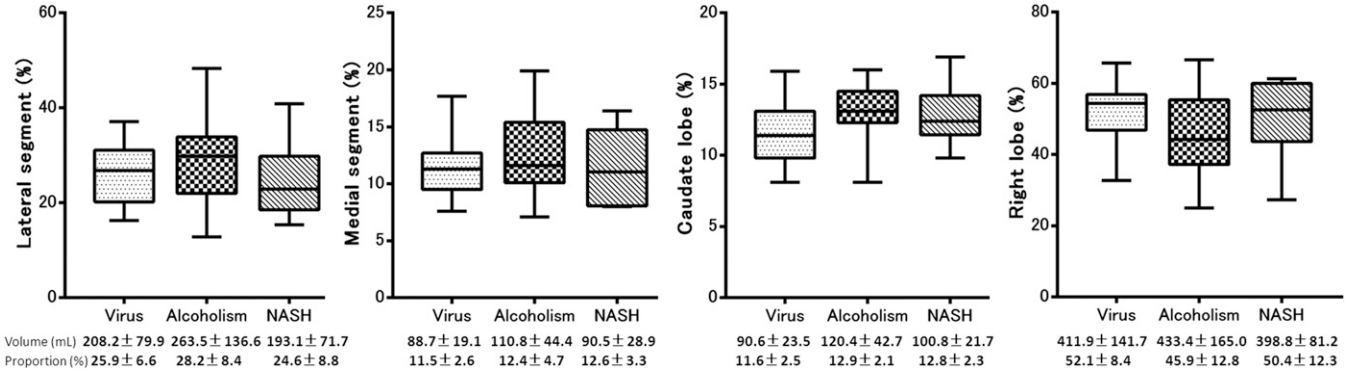

Figure 7. Comparison of portal phase of axial CT images in a 59-year-old man with virus-related cirrhosis (a), in a 53-year-old man with alcoholic cirrhosis (b) and in a 56-year-old woman with non-alcoholic steatohepatitis (NASH)-related cirrhosis (c) in Child–Pugh Class C. Whole liver shows diffuse atrophy in all aetiologies, and cirrhosis caused by all aetiologies displayed atrophy of the medial segment (white asterisks), right lobe (white dots) and hypertrophy of lateral segment (black asterisks) and caudate lobe (black dots). These morphometric changes tended to be similar among the three aetiologies, and no segments showed significant differences among them.

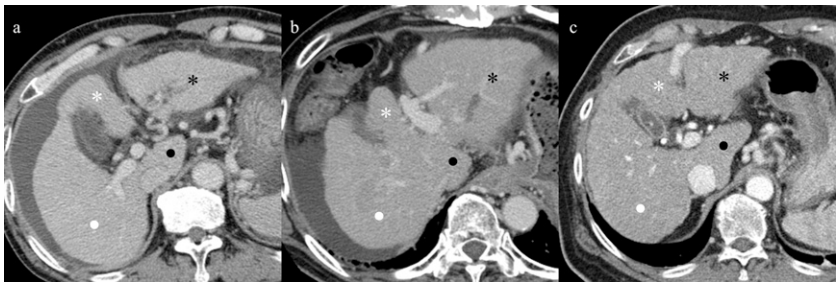

of another area. However, as cirrhosis progresses, the characteristic histological features of various aetiologies may be lost, and the features of specific types of cirrhosis may become indistinguishable from cirrhosis owing to other causes.[29] In addition, the hypertrophic area cannot compensate for the atrophic area, and the whole liver eventually shows atrophy in advanced cirrhosis as shown previously[5–7] and in our study. Therefore, the magnitude of the differences between aetiologies would decrease with progression of cirrhosis as shown in our study, although there were no baseline scans of the patients in different stages of cirrhosis.

This study has several limitations. First, the determination of the exact boundary of each area was not always accurate, although, volumetry based on MDCT is currently the most reliable method.[6,7,19,20] Second, the number of subjects was small, especially in patients with Child–Pugh Class C. Third, some of the patients with cirrhosis were not included because of a low contrast between liver parenchyma and hepatic vessels and/or a history of treated hepatocellular carcinoma. Fourth, we analysed only three aetiologies, and further analysis of other types of cirrhosis may be necessary to better understand the entire spectrum of morphometric changes. Fifth, we analysed only from the viewpoint of intrahepatic morphometric changes. However, various extrahepatic changes such as splenomegaly, the presence of varices or collaterals and ascites may help in the determination of the stage of cirrhosis as well. Sixth, the morphometric analysis was done using a time-consuming software and technique, which is not used in clinical practice. Therefore, further evaluation of this morphometric changes needs to be assessed in an easily available clinical setting to identify whether this can be used a clinical tool.

In conclusion, morphometric changes of cirrhosis display different patterns according to underlying aetiology. Differences between aetiologies would decrease with progression of cirrhosis. Understanding the different morphological patterns may help to frame further studies aimed to evaluate the alterations in vascular supply/drainage that occur with cirrhosis.

ACKNOWLEDGMENTS

We deeply appreciate the statistical support of Dr Takayuki Abe (Center for Clinical Research, Keio University School of Medicine, Tokyo, Japan) in our study.

FUNDING

Supported in part by a Grant-in-Aid for Young Scientists (B) (JSPS KAKENHI Grant Number 26860539).

REFERENCES

1. National Institutes of Health. National Institutes of Health Consensus Development Conference statement: management of hepatitis C: 2002—June 10–12, 2002. *Hepatology* 2002; **36**: S3–S20.
2. Bravo AA, Sheth SG, Chopra S. Liver biopsy. *N Engl J Med* 2001; **344**: 495–500. doi: 10.1056/NEJM200102153440706
3. Piccinino F, Sagnelli E, Pasquale G, Giusti G. Complications following percutaneous liver biopsy: a multicentre retrospective study on 68,276 biopsies. *J Hepatol* 1986; **2**: 165–73. doi: 10.1016/S0168-8278(86)80075-7
4. Regev A, Berho M, Jeffers LJ, Milikowski C, Molina EG, Pyrsopoulos NT, et al. Sampling error and intraobserver variation in liver biopsy in patients with chronic HCV infection. *Am J Gastroenterol* 2002; **97**: 2614–8. doi: 10.1111/j.1572-0241.2002.06038.x
5. Ito K, Mitchell DG, Hann HW, Outwater EK, Kim Y, Fujita T, et al. Progressive viral-induced cirrhosis: serial MR imaging findings and clinical correlation. *Radiology* 1998; **207**: 729–35. doi: 10.1148/radiology.207.3.9609897
6. Ozaki K, Matsui O, Kobayashi S, Sanada J, Koda W, Minami T, et al. Selective atrophy of the middle hepatic venous drainage area in hepatitis C-related cirrhotic liver: morphometric study by using multidetector CT. *Radiology* 2010; **257**: 705–14. doi: 10.1148/radiol.10100468
7. Zhou XP, Lu T, Wei YG, Chen XZ. Liver volume variation in patients with virus-induced cirrhosis: findings on MDCT. *AJR Am J Roentgenol* 2007; **189**: 153–9. doi: 10.2214/AJR.07.2181

8. Harbin WP, Robert NJ, Ferrucci JT Jr. Diagnosis of cirrhosis based on regional changes in hepatic morphology: a radiological and pathological analysis. *Radiology* 1980; **135**: 273–83. doi: 10.1148/radiology.135.2.7367613
9. Giorgio A, Amoroso P, Lettieri G, Fico P, de Stefano G, Finelli L, et al. Cirrhosis: value of caudate to right lobe ratio in diagnosis with US. *Radiology* 1986; **161**: 443–5. doi: 10.1148/radiology.161.2.3532188
10. Torres WE, Whitmire LF, Gedgaudas-McClees K, Bernardino ME. Computed tomography of hepatic morphologic changes in cirrhosis of the liver. *J Comput Assist Tomogr* 1986; **10**: 47–50. doi: 10.1097/00004728-198601000-00009
11. Ito K, Mitchell DG, Gabata T, Hussain SM. Expanded gallbladder fossa: simple MR imaging sign of cirrhosis. *Radiology* 1999; **211**: 723–6. doi: 10.1148/radiology.211.3.r99ma31723
12. Ito K, Mitchell DG, Gabata T. Enlargement of hilar periportal space: a sign of early cirrhosis at MR imaging. *J Magn Reson Imaging* 2000; **11**: 136–40. doi: 10.1002/(SICI)1522-2586(200002)11:2<136::AID-JMRI9>3.0.CO;2-B
13. Awaya H, Mitchell DG, Kamishima T, Holland G, Ito K, Matsumoto T. Cirrhosis: modified caudate-right lobe ratio. *Radiology* 2002; **224**: 769–74. doi: 10.1148/radiol.2243011495
14. Ito K, Mitchell DG, Kim MJ, Awaya H, Koike S, Matsunaga N. Right posterior hepatic notch sign: a simple diagnostic MR finding of cirrhosis. *J Magn Reson Imaging* 2003; **18**: 561–6. doi: 10.1002/jmri.10387
15. Okazaki H, Ito K, Fujita T, Koike S, Takano K, Matsunaga N. Discrimination of alcoholic from virus-induced cirrhosis on MR imaging. *AJR Am J Roentgenol* 2000; **175**: 1677–81. doi: 10.2214/ajr.175.6.1751677
16. Couinaud C. *Surgical anatomy of the liver revisited*. Paris, France: Couinaud; 1989. pp. 96–124.
17. Abdalla EK, Vauthey JN, Couinaud C. The caudate lobe of the liver: implications of embryology and anatomy for surgery. *Surg Oncol Clin N Am* 2002; **11**: 835–48. doi: 10.1016/S1055-3207(02)00035-2
18. DuBois DF, DuBois EF. A formula to estimate the approximate surface area if height and weight be known. *Arch Intern Med* 1989; **5**: 303–13.
19. Saito S, Yamanaka J, Miura K, Nakao N, Nagao T, Sugimoto T, et al. A novel 3D hepatectomy simulation based on liver circulation: application to liver resection and transplantation. *Hepatology* 2005; **41**: 1297–304. doi: 10.1002/hep.20684
20. Frericks BB, Kirchhoff TD, Shin HO, Stamm G, Merkesdal S, Abe T, et al. Preoperative volume calculation of the hepatic venous draining areas with multi-detector row CT in adult living donor liver transplantation: impact on surgical procedure. *Eur Radiol* 2006; **16**: 2803–10. doi: 10.1007/s00330-006-0274-6
21. Bolognesi M, Sacerdoti D, Mescoli C, Bombonato G, Cillo U, Merenda R, et al. Different hemodynamic patterns of alcoholic and viral endstage cirrhosis: analysis of explanted liver weight, degree of fibrosis and splanchnic Doppler parameters. *Scand J Gastroenterol* 2007; **42**: 256–62. doi: 10.1080/00365520600880914
22. Faria SC, Ganesan K, Mwangi I, Shiehmorteza M, Viamonte B, Mazhar S, et al. MR imaging of liver fibrosis: current state of the art. *Radiographics* 2009; **29**: 1615–35. doi: 10.1148/rg.296095512
23. Portmann B, Nakanuma Y. Diseases of the bile ducts. In: MacSween RNM, Burt AD, Portmann BC, Ishak KG, Scheuer PJ, Anthony PP, eds. *Pathology of the liver*. 4th edn. London, UK: Churchill Livingstone; 2002. pp. 435–506.
24. Pinto HC, Baptista A, Camilo ME, Valente A, Saragoça A, de Moura MC. Nonalcoholic steatohepatitis. Clinicopathological comparison with alcoholic hepatitis in ambulatory and hospitalized patients. *Dig Dis Sci* 1996; **41**: 172–9. doi: 10.1007/BF02208601
25. Maher JJ. Hepatic fibrosis caused by alcohol. *Semin Liver Dis* 1990; **10**: 66–74. doi: 10.1055/s-2008-1040458
26. Ohtomo K, Baron RL, Dodd GD III, Federle MP, Miller WJ, Campbell WL, et al. Confluent hepatic fibrosis in advanced cirrhosis: appearance at CT. *Radiology* 1993; **188**: 31–5. doi: 10.1148/radiology.188.1.8511316
27. Bilaj F, Hyslop WB, Rivero H, Firat Z, Vaidean G, Shrestha R, et al. MR imaging findings in autoimmune hepatitis: correlation with clinical staging. *Radiology* 2005; **236**: 896–902. doi: 10.1148/radiol.2363041262
28. Blachar A, Federle MP, Brancatelli G. Primary biliary cirrhosis: clinical, pathologic, and helical CT findings in 53 patients. *Radiology* 2001; **220**: 329–36. doi: 10.1148/radiology.220.2.r01au36329
29. Wallace K, Burt AD, Wright MC. Liver fibrosis. *Biochem Genet* 2008; **411**: 1–18. doi: 10.1042/BJ20071570
30. Brown JJ, Naylor MJ, Yagan N. Imaging of hepatic cirrhosis. *Radiology* 1997; **202**: 1–16. doi: 10.1148/radiology.202.1.8988182